WATER RESOURCES RESEARCH, VOL. 49, 5462–5472, doi:10.1002/wrcr.20417, 2013

Geomorphic signatures on Brutsaert base flow recession analysis

Raphaël Mutzner,[1] Enrico Bertuzzo,[1] Paolo Tarolli,[2] Steven V. Weijs,[1] Ludovico Nicotina,[1,3] Serena Ceola,[1,4] Nevena Tomasic,[1] Ignacio Rodriguez-Iturbe,[5] Marc B. Parlange,[1] and Andrea Rinaldo[1,6]

Received 4 January 2013; revised 4 June 2013; accepted 12 July 2013; published 6 September 2013.

[1] This paper addresses the signatures of catchment geomorphology on base flow recession curves. Its relevance relates to the implied predictability of base flow features, which are central to catchment-scale transport processes and to ecohydrological function. Moving from the classical recession curve analysis method, originally applied in the Finger Lakes Region of New York, a large set of recession curves has been analyzed from Swiss streamflow data. For these catchments, digital elevation models have been precisely analyzed and a method aimed at the geomorphic origins of recession curves has been applied to the Swiss data set. The method links river network morphology, epitomized by time-varying distribution of contributing channel sites, with the classic parameterization of recession events. This is done by assimilating two scaling exponents, β and b_G, with $|\mathrm{d}Q/\mathrm{d}t| \propto Q^{\beta}$ where Q is at-a-station gauged flow rate and $\mathrm{N}(l) \propto \mathrm{G}(l)^{b_G}$ where l is the downstream distance from the channel heads receding in time, $\mathrm{N}(l)$ is the number of draining channel reaches located at distance l from their heads, and $\mathrm{G}(l)$ is the total drainage network length at a distance greater or equal to l, the active drainage network. We find that the method provides good results in catchments where drainage density can be regarded as spatially constant. A correction to the method is proposed which accounts for arbitrary local drainage densities affecting the local drainage inflow per unit channel length. Such corrections properly vanish when the drainage density become spatially constant. Overall, definite geomorphic signatures are recognizable for recession curves, with notable theoretical and practical implications.

Citation: Mutzner, R., E. Bertuzzo, P. Tarolli, S. V. Weijs, L. Nicotina, S. Ceola, N. Tomasic, I. Rodriguez-Iturbe, M. B. Parlange, and A. Rinaldo (2013), Geomorphic signatures on Brutsaert base flow recession analysis, *Water Resour. Res.*, *49*, 5462–5472, doi:10.1002/wrcr.20417.

1. Introduction

[2] Groundwater is the main contributor of a river catchment's base flow whose predictability during recession events is of crucial importance for water resource management. Recession curves have been widely studied in the past and their characteristics used to establish basin-scale parameters (see *Tallaksen* [1995] for a review). In particular, *Brutsaert and Nieber* [1977] analyzed daily discharge values of six basins in the Finger Lakes region of the northeastern US and proposed an analytical tool to characterize the recession flow based on the description of the discharge change rate dQ/dt as a function of the discharge Q. Unlike many nonlinear recession flow models, this method avoids the knowledge of the precise beginning of the recession event which can be difficult to evaluate due to the continuous nature of streamflow measurements. The main feature of their method is the comparison of the observations with analytical solutions of the Boussinesq equation for an unconfined rectangular aquifer under particular boundary conditions. Two exact solutions of the Boussinesq equation [*Boussinesq*, 1904; *Polubarinova-Kochina*, 1962] and an approximated linearized solution [*Boussinesq*, 1903] can be expressed in the form:

$$\frac{dQ}{dt} = -kQ^{\beta} \tag{1}$$

where β and k are constants depending on the flow regime considered. In order to avoid contributions from relatively fast subsurface flow, overland flow, and evapotranspiration, *Brutsaert and Nieber* [1977] recommended the use of the lower envelope of the point cloud in the $\ln(-dQ/dt)$ versus $\ln Q$ plot, corresponding to the slowest recession rate. Based on their study, they identified two typical values of β, describing the rate of decline in streamflow recessions: $\sim$1.5 for low Q (long-term response) and $\sim$3 for high Q (short-term response). Moreover, some parameters of the

[1]School of Architecture, Civil and Environmental Engineering, École Polytechnique Fédérale de Lausanne, Lausanne, Switzerland.
[2]Department of Land, Environment, Agriculture and Forestry, University of Padua, Padua, Italy.
[3]Risk Management Solutions Ltd., London, UK.
[4]Department DICAM, University of Bologna, Bologna, Italy.
[5]Department of Civil and Environmental Engineering, Princeton University, Princeton, New Jersey, USA.
[6]Dipartimento ICEA, University of Padua, Padua, Italy.

Corresponding author: R. Mutzner, School of Architecture, Civil and Environmental Engineering, École Polytechnique Fédérale de Lausanne, Station 2, CH-1015, Lausanne, Switzerland. (raphael.mutzner@epfl.ch)

0043-1397/13/10.1002/wrcr.20417

watershed such as the saturated hydraulic conductivity stemming from the Boussinesq equation have been computed from the intercept of the $\ln(-dQ/dt)$ versus $\ln Q$ plot.

[3] The method has been widely applied to estimate basin-scale parameters in relatively natural areas [*Brutsaert and Lopez*, 1998; *Brutsaert and Sugita*, 2008; *Brutsaert and Hiyama*, 2012; *Eng and Brutsaert*, 1999; *Malvicini et al*., 2005; *Mendoza et al*., 2003; *Parlange et al*., 2001; *Szilagyi et al*., 1998; *Troch et al*., 1993; *Vogel and Kroll*, 1992; *Zecharias and Brutsaert*, 1988] and in engineered catchments [*Rupp et al*., 2004; *Wang and Cai*, 2010], to formulate base flow in a watershed model [*Szilagyi and Parlange*, 1999], in order to separate the base flow [*Szilagyi and Parlange*, 1998] or to assess long-term groundwater storage changes [*Brutsaert*, 2008]. *Rupp and Selker* [2006a, 2006b] showed some limitations of the method, e.g., in the case of sloping aquifers. Recession curve studies moving from *Brutsaert and Nieber*'s [1977] work have proved of central importance in a broad range of topics ranging from comprehensive water resource management to studies on fluvial biodiversity, catchment-scale transport, ecohydrology, and the so-called old-water paradox [*Bertuzzo et al*., 2007; *Botter et al*., 2007a, 2007b, 2009, 2010; *Ceola et al*., 2010; *Harman et al*., 2009; *Kirchner*, 2009; *Kondolf et al*., 1987; *Palmroth et al*., 2010; *Rinaldo et al*., 1995a, 1995b, 2006, 2011; *Rodriguez-Iturbe et al*., 2009; *Tague and Grant*, 2004; *Thompson and Katul*, 2012; *Wittenberg*, 1999; *Zaliapin et al*., 2010].

[4] Recently, several studies [*Biswal and Marani*, 2010; *Biswal and Nagesh Kumar*, 2012; *McMillan et al*., 2011; *Rupp et al*., 2009; *Shaw and Riha*, 2012] analyzed the recession events on a seasonal or event-based time scale and discussed their shifts in the $\ln(-dQ/dt)$ versus $\ln Q$ plot, linking them to different antecedent soil moisture and evapotranspiration happening over the season. In particular, *Biswal and Marani* [2010], *Biswal and Nagesh Kumar* [2012], and *Shaw and Riha* [2012] proposed to obtain the parameters β and k of equation (1) by fitting a linear model to every recession event in order to obtain a distribution of the parameters instead of fitting a line to the lower envelope of the point cloud. With this method, the authors found that the slopes of the individual recession curves, i.e., the parameter β, were in general larger than the one of the lower envelope, resulting in an underestimation of the streamflow decline rate when described by a unique $dQ/dt - Q$ relationship. Moreover, *Biswal and Marani* [2010] proposed to link recession event parameterization to river morphology through a time-varying geometry of saturated channel sites. In particular, they developed a theory based on geomorphological arguments to link the exponent β of equation (1) to that characterizing an empirical relation resulting from the analysis of Digital Elevation Models (DEM). In this model, the variation of the discharge is linked to the direct drainage into a time-varying Active Drainage Network (ADN). When the recession hydrograph at an outlet is dominated by drainage of the unconfined aquifer as in *Brutsaert and Nieber* [1977], the ADN is the length of the channel network instantaneously intersecting it. The model relies on four main assumptions. First, the authors assume that the recession flow could be studied as a succession of steady flows since the time scale at which the discharge varies is much longer than the time scale of water propagating in the network. Second, by assuming a spatially constant discharge per unit length q_L, the total discharge $Q(t)$ can be expressed as:

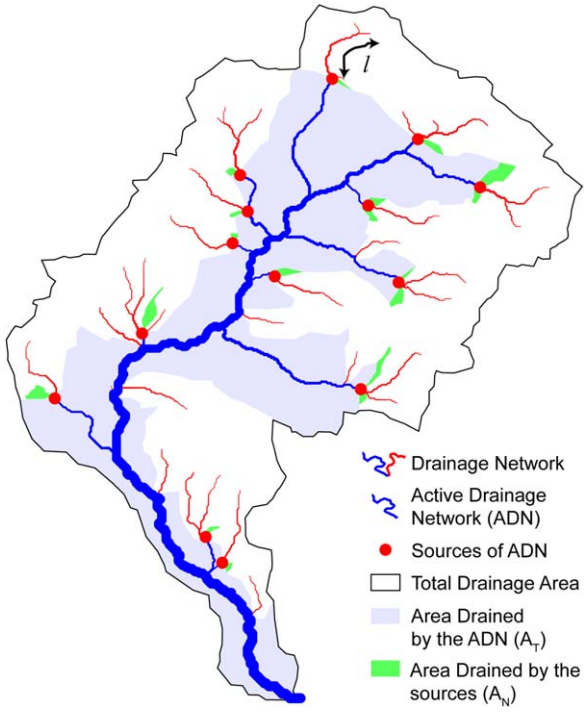

Figure 1. Idealized example of a recession described by the geomorphological conceptual models. The Active Drainage Network (ADN) is represented in blue solid lines and the dry part of the ADN is represented in red solid lines. The sources (here $N = 14$) are represented in red solid circles, the blue shaded area represents the fraction of the basin drained by the ADN (A_T).

$$Q(t) = q_L(t)G(l(t)) \tag{2}$$

where $G(l(t))$ is the total length of the drainage network actively contributing at time t and $l(t)$ is the distance between the actual source of the ADN and their location at the beginning of the recession event (Figure 1). Third, they assume that all sources of the ADN recede at the same speed $c = dl/dt$, constant in space and time such that the change in time of the network length is proportional to the number of sources N ($dG/dt = dG/dl \cdot dl/dt \propto N \cdot c$). Equation (2) can be differentiated in time:

$$\frac{dQ(t)}{dt} = -q_L(t)cN(t) + \frac{dq_L(t)}{dt}G(t) \tag{3}$$

where the third assumption has been employed. The first term at right-hand side of equation (3) embeds the geomorphologic signature and the second the Brutsaert recession proper. Fourth, they studied the case where the variation in time of the ADN, assumed to be much larger than the variation in time of the discharge per unit length, dominates the second term in equation (3) which can thus be neglected. This work has clearly established that base flow recession

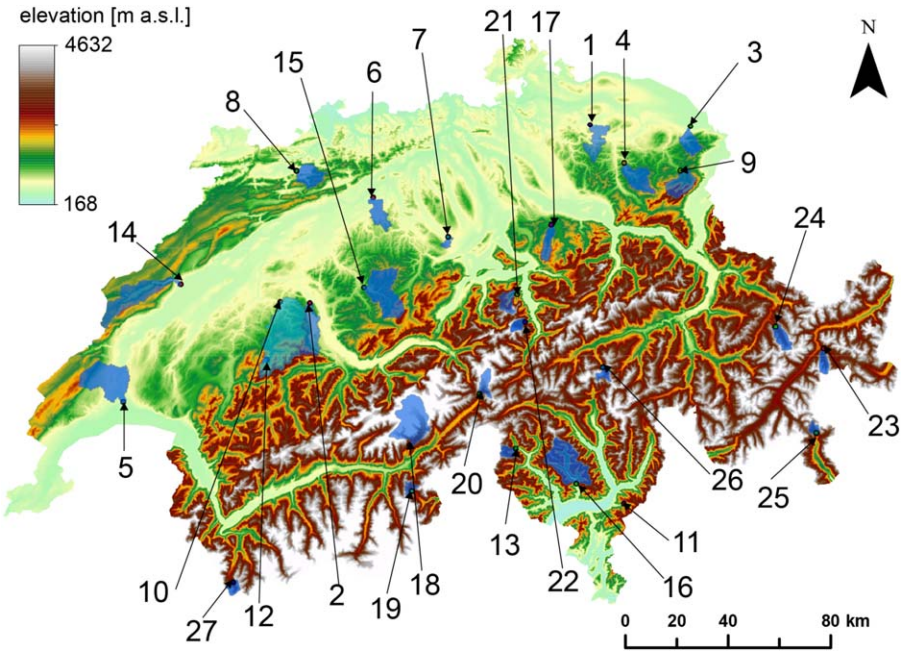

Figure 2. Map of the experimental catchments used in this study. Some geomorphologic characteristics and description of the available data are listed in Table 1.

curves bear the signatures of the geomorphological structure of the contributing river basin.

[5] However, the innovative method proposed by *Biswal and Marani* [2010] postulates constant drainage density, classically defined as the total length of stream channels divided by the area they drain [*Horton*, 1932, 1945] and properly described by a random space function endowed with spatial correlation [*Tucker et al*., 2001]. Other formulations have also been proposed [*Marani et al*., 2003] as it was shown that networks with the same Hortonian drainage density may embed rather different distributions of unchanneled pathways, and thus different extents of the actual density of the drainage network. Random functions are defined by the statistical properties of the length of the (steepest-descent) distance from any unchanneled site to the first occurrence of a stream channel [*Tucker et al*., 2001]. The consequences are far from obvious. In fact, the Hortonian definition applies reasonably well only in cases where locally the mean unchanneled lengths vary little from subcatchment to subcatchment, thus postulating that channel initiation processes are homogeneous—technically, whenever automatic network extractions assume it, like, e.g., in the case of constant support area (for a review see e.g. *Rodriguez-Iturbe and Rinaldo* [2001]). This is seldom the case in nature [e.g., *Montgomery and Dietrich*, 1988, 1992]. Typically, in proglacial catchments, mean unchanneled distances exhibit a broad range varying from tens of meters in shallow-soiled topographically concave source areas to a few km in deep moraines [e.g., *Montgomery and Foufoula-Georgiou*, 1993; *Tarolli and Dalla Fontana*, 2009]. Thus, one wonders whether the geomorphic framework proposed by *Biswal and Marani* [2010] for predicting the shape of Brutsaert recession curves can be suitably generalized to account for spatially uneven drainage densities. In practice, one needs to relax certain assumptions therein and check empirically whether geomorphic signatures could still be interpreted in such context, possibly improving the explanatory power of the original method and reducing to it in the limit case of constant drainage density. This is precisely what this paper addresses.

2. Study Areas and Available Data

[6] We analyze 26 catchments located in Switzerland (Figure 2) presenting different sizes, relief, slope, and soil properties. The watersheds are all characterized by relatively little anthropogenic influence on the streamflow behavior. The hourly averaged streamflow data of the 26 gauging stations are obtained from the Swiss Federal Office for the Environment. The rainfall data is obtained through SwissMetNet, a network of automatic weather stations operated by MeteoSwiss. All the stations are measuring the precipitation within a maximum radius of 10 km from the corresponding discharge gauging station. The DEM of the 26 basins were extracted from a 25 m resolution DEM of Switzerland provided by the Swiss Federal Office of Topography with standard commercial geographic information system (GIS) software. Table 1 summarizes the principal characteristics of the 26 catchments.

[7] We also analyze the Val Ferret catchment (catchment 27 in Table 1), an experimental site we have monitored since 2008 [see *Simoni et al*., 2011; *Tobin et al.*, 2013]. Streamflow data are available every 5 min and obtained through water level measurements and a rating curve that was derived using the salt-dilution method on a yearly basis for the period 2008–2012. Recently, *Weijs et al*. [2013] decreased the error on the rating curve by combining the water level with the natural electrical conductivity of stream water which appears particularly useful for Alpine

Table 1. Summary of Geomorphological Characteristics, Discharge, and Precipitation Data for the 27 Watersheds[a]

		Geomorphology					Discharge Data				Precipitation Data			
Number of Basin	Name	Basin Surface (km^2)	Mean Basin Altitude (m)	Max Basin Altitude (m)	Mean Basin Slope (m/km)	Glacier Ext. (%)	Coordinates Gauging Station X,Y		Station Altitude (m)	Measure Start	Name	Coordinates Precipitation Station X,Y		Distance from Discharge Station (km)
1	Murg-Wängi	78	650	1035	25.5	0	714,105	261,720	466	1 Jan 1974	Eschlikon	715,095	258,260	3.60
2	Gürbe-Belp, Mülimatt	117	849	2176	52.2	0	604,810	192,680	522	1 Jan 1974	Belp	605,140	193,805	1.17
3	Goldach Bleiche	49.8	833	1251	39.3	0	753,190	261,590	399	1 Jan 1974	Arbon	749,840	263,150	3.70
4	Necker-Mogelsberg- Aachsäge	88.2	959	1532	35.6	0	727,110	247,290	606	1 Jan 1974	Mogelsberg	728,220	247,010	1.14
5	Venoge-Ecublens, Les bois	231	700	1431	20.8	0	532,040	154,160	383	1 Jan 1979	Marcelin	527,060	152,160	5.37
6	Murg-Walliswil	207	637	1119	18.6	0	629,340	233,555	419	1 Jun 1980	Wynau	626,400	233,850	2.95
7	Sellenbodenbach-Neuenkirch	10.5	615	838	36.5	0	658,530	218,290	515	1 Sep 1990	Sempach	657,010	220,940	3.05
8	Scheulte-Vicques	72.8	785	1302	30.9	0	599,485	244,150	463	01.01.1992	Mervelier	604,610	243,670	5.15
9	Sitter-Appenzell	74.2	1252	2500	139.6	0.08	749,040	244,220	769	1 Jan 1974	Appenzell	747,735	244,475	1.33
10	Sense-Thörishaus-Sensematt	352	1068	2190	25.4	0	593,350	193,020	553	1 Jan 1977	Schwarzenburg	593150	184720	8.30
11	Melera-Melera	1.05	1419	1728	71.1	0	726,988	114,670	944	1 Jan 1974	Bellinzona	721,060	116,800	6.30
12	Rotenbach-Schweinsberg	1.65	1454	1628	151.3	0	587,980	170,590	1275	1 Aug 1995	Sangernboden	593,220	173,905	6.20
13	Riale di Calneggia-Pontit	24	1996	2921	231	0	684,970	135,970	890	1 Jan 1974	Bosco-	681,160	130,025	7.06
14	Areuse-Boudry	377	1060	1607	27.3	0	554,350	199,940	444	1 Jan 1983	Combe-	551,220	201,450	3.48
15	Ilfis-Langnau	188	1051	2092	30.9	0	627,320	198,600	685	1 Apr 1989	Kurzeneialp	630,575	207,010	9.02
16	Verzasca-Campiol	185	1661	2864	72.4	0	708,420	122,290	490	1 Aug 1989	Cimetta	704,370	117,515	6.26
17	Alp-Einsiedeln	46.4	1155	1899	40.8	0	698,640	223,020	840	1 Feb 1991	Altmatt	695,420	220,770	3.93
18	Massa-Blatten bei Naters	195	2945	4195	183.2	65.9	643,700	137,290	1446	1 Jan 1974	Brig	640,570	129,080	8.79
19	Krummbach-Klusmatten	19.8	2276	3268	121.8	3	644,500	119,420	1795	1 Jan 1974	Simplon-	647,570	116,110	4.51
20	Rhone-Gletsch	38.9	2719	3622	74.2	52.2	670,810	157,200	1761	1 Jan 1974	Grimsel	668,583	158,215	2.45
21	Grosstalbach – Isenthal	43.9	1820	2952	211.1	9.3	685,500	196,050	767	1 Jan 1974	Isenthal	685,460	196,110	0.07
22	Alpbach-Erstfel- Bodenberg	20.6	2200	3198	414	27.7	688,560	185,120	1022	1 Jan 1974	Altdorf	690,174	193,558	8.59
23	Ova da Cluozza-Zernez	26.9	2368	3165	180	2.2	804,930	174,830	1509	1 Jan 1974	Zernez	802,720	175,230	2.25
24	Dischmabach – Davos	43.3	2372	3146	129.4	2.1	786,220	183,370	1668	1 Jan 1974	Dischma	786,600	182,990	0.54
25	Poschiavin-La Rösa	14.1	2283	3032	91.3	0.35	802,120	132,010	1860	1 Jan 1974	Cavaglia	799,850	138,470	4.21
26	Rein da Sumvitg,Encardens	21.8	2450	3168	165.5	6.7	718,810	167,690	1490	1 Jan 1977	Vrin	727,220	168,670	8.47
27	Val Ferret, Ferret	20.4	2422.8	3206	385	2.1	574,932	83,779	1173	1 May 2008	Val Ferret	Various	Various	Various

[a]The coordinates are given in the Swiss Coordinate System.

watersheds. The rainfall data for the Val Ferret catchment is obtained along with other forcing parameters by a wireless network of up to 26 small meteorological stations deployed on representative sites of the catchment [*Simoni et al*., 2011]. For this catchment, we used both a 5 m resolution light detection and ranging (LiDAR)-derived DEM and the 25 m resolution DEM provided by the Swiss Federal Office of Topography. Moreover, the actual channel network of the Val Ferret catchment has been surveyed by Differential Global Positioning System during an extensive field campaign in 2011.

3. Methods

[8] In order to compute the recession exponents, measured discharge has been averaged from hourly values to daily values in order to filter out the diurnal contributions of snow or icemelt to the streamflow daily periodicity. Precipitation has been integrated over the same period and used to define recession events as 6 consecutive days without precipitation. Moreover, following *Biswal and Marani* [2010], we only considered events with peak discharge larger than the average discharge in order to enhance the geomorphic signature on the base flow recession and to insure that the whole catchment is active at the onset of recession—unlike the original method from *Brutsaert and Nieber* [1977] where the focus was on the groundwater hydraulics signature. The discharge variations and values have been computed as $-dQ/dt = (Q_t - Q_{t+\Delta t})/\Delta t$ and $Q = (Q_t + Q_{t+\Delta t})/2$ following *Brutsaert and Nieber* [1977], where Δt is the time step of 1 day used in the analysis. Recession events with nonmonotonically decreasing discharge values were discarded from the analysis (i.e., events containing days with $dQ/dt \geq 0$ were removed from the analysis). In the log-log plot, the single $-dQ/dt$ versus Q curves tend to be shifted depending on the maximum peak discharge, antecedent soil moisture and evapotranspiration. According to *Biswal and Marani* [2010], *Biswal and Nagesh Kumar* [2012], and *Shaw and Riha* [2012], a value of the exponent β is obtained for every recession event by fitting a linear model in the log-log space using ordinary least squares. In the following, we will refer to the recession exponent β of a catchment as the median of the exponent β's frequency distribution. This event-based approach differs from the previous studies linking the analyzed recession discharges based on a one-to-one relationship between the amount of water stored in the catchment and the discharge occurring during recessions.

[9] The variables $N(t)$ and $G(t)$, instrumental for the geomorphological analysis, can be obtained from the analysis of DEMs by extracting the channel network on the basis of standard topographic threshold methods [*O'Callaghan and Mark*, 1984; *Tarboton et al*., 1991] or slope-dependent or topographic curvature-dependent support areas mimicking different channel initiation processes [*Montgomery and Dietrich*, 1988, 1992; *Montgomery and Foufoula-Georgiou*, 1993; *Sofia et al*., 2011; *Tarolli and Dalla Fontana*, 2009], the latter being capable of rendering spatially heterogeneous drainage densities. As done in *Biswal and Marani* [2010], we use a simple flow accumulation threshold as channel network extraction method to standardize procedures, except for the case where ground truthing was available (for catchment 27, see section 2). After a certain time t, the number of sources $N(t)$ is determined by the number of reaches located at distance $l = c(t - t_o)$ from their farthest upstream initial source (Figure 1). Under the assumption that the ADN varies quickly, such that the term in dq_L/dt can be neglected, one has $dQ/dt \propto -N(t)$ from equation (3) and $Q \propto \mathrm{G}(t)$ from equation (2). Inserting these two relations in equation (1), one finally has

$$N(l) \propto G(l)^{b_G} \tag{4}$$

where $b_G = \beta$ if the geomorphological exponent correctly captures the exponent obtained from the analysis of the recession curves.

[10] In this work, we propose a revised approach of the conceptual model developed in *Biswal and Marani* [2010]. We assume that the directly contributing discharge Q is drawn not from an unconfined aquifer like in the traditional way but in our case by the unchanneled area draining directly in the ADN:

$$Q(t) = \sum_{i \in ADN(t)} a_i q_i \sim q \sum_{i \in ADN(t)} a_i \propto \sum_{i \in ADN(t)} a_i = A_T(t) \tag{5}$$

where ADN is the Active Drainage Network at time t, A_T is the area draining directly in the ADN, a_i is the directly contributing area at site i and q_i is the discharge per pixel at site i, see Figure 1. The second approximation derives from assuming q constant as done in *Biswal and Marani* [2010]. As such we assume that the variation of the contributing discharge is proportional to the rate of change in directly contributing area therein and hence on local drainage density in the sense of *Tucker et al*. [2001]:

$$\frac{dQ}{dt} \propto \frac{d}{dl}\left(\sum_{i \in ADN(t)} a_i\right)\frac{dl}{dt} \propto c\frac{d}{dl}\sum_{i \in ADN(t)} a_i = c\frac{dA_T}{dl} \tag{6}$$

where c is the speed at which the sources recede, assumed constant in space and time as in a negative traveling wave. The approach is thus based on the computation of the direct drainage areas of the ADN. Moreover, the change in direct drainage area is given by the area A_N draining directly in the sources of the ADN at time t:

$$\frac{dA_T}{dl} \propto A_N(l) \tag{7}$$

[11] Combining equations (1), (5), (6), and (7), we obtain similarly to equation (4):

$$A_N \propto {A_T}^{b_A} \tag{8}$$

where $b_A = \beta$ if the geomorphological exponent obtained with the new method matches the exponent obtained from the analysis of the recession curves. In this study, we propose to compute the geomorphological exponents b_G of equation (4) and b_A of equation (8) for the 27 watersheds considered and to compare them with the values of the recession exponent β obtained from the recession analysis. Then, we study the differences between the two methods in

terms of mean catchment altitude, aiming at improving our understanding of the geomorphological origin of the recession curves.

4. Results

[12] Examples of three catchments (basins 15, 25, and 27, see Table 1 for geomorphological characteristics), where the two different methods have been applied are shown in Figure 3. The examples present different cases and results characteristic of the correction we propose in this work. The channel network has been suitably extracted from the DEM using a flow accumulation threshold of 100 pixels and is here color coded in blue in Figure 3a. Different flow accumulation threshold values and another channel network extraction method (depending on a slope-area threshold) have been used without appreciable changes in the following results. For the study of the Val Ferret catchment (watershed 27 in Table 1), the monitored network (see section 2) has been used as the basis for the determination of the ADN. The distribution of the distance from any unchanneled site to its nearest stream channel following the steepest path has been studied in relevant subcatchments of the watersheds. It appears that the hillslope distance to the nearest channel and therefore the local drainage density [*Tucker et al*., 2001] cannot be considered constant in most high mountain catchments and especially in the case of the Val Ferret catchment where the real monitored network has been used.

[13] The recession slope analysis has been carried out for each of the 27 basins by fitting each recession event separately with least squares and by computing the frequency distribution of the β values. Some examples of individual fits are color coded in Figure 3b, along with the cloud of points obtained for all the events (gray dots). The solid black line represents the fit of all the events. As expected, the exponent β of equation (1) obtained with the global fit is less than the average of the coefficients fitted on single events. The results of the recession slope analysis are presented in Table 2. In the following, the values of a catchment's median exponent β are used as a comparative basis for the scaling exponents b_G and b_A of the different geomorphological models. Note that, in general, the standard deviations of the exponent β are relatively large due to the inferences of fast responses of the catchments to precipitation or glacier melts. The low extreme ($\beta = 1.06$, basin 20, see in Table 2) corresponds to a largely glaciated, high-altitude catchment whereas the high extreme ($\beta = 6.24$, basin 6, Table 2) corresponds to a highly urbanized catchment. Both cases have been discarded in the following calculations.

[14] The comparison of the two models is shown in Figure 3c, as per the method developed in *Biswal and Marani* [2010], we show the number of sources N plotted versus the total length G of the ADN. As postulated by the original method, the number of sources decreases or stays constant in time, resulting in a monotonically decreasing function $N(G)$. The plots result in a piecewise constant function at low values of the network length since low-order channels have dried out already so that the ADN stems mainly from high-order streams. In order to better estimate the geomorphological parameters b_G and b_A, the data have been fitted only up to when 80% of the initial ADN has receded in order to avoid the last part where $N(G)$ is piecewise constant. In Figure 3d, according to the proposed revision of the original method, we show the area A_N draining directly in the sources of the ADN versus the total area A_T draining in the ADN. In the three plots, the cloud of points is quite noisy at the end of the recession (that is, for the smallest total areas) which is a signature of the watershed geometrical attributes and of uneven local drainage densities. All the values of the exponents b_G and b_A are presented in Table 2. The two exponents b_G and b_A are similar in the case of catchment 15 (first column in Figure 3), a catchment with fairly constant hillslope to channel distance. This supports our ansatz that the different methods provide indistinguishable results in cases where drainage density can be regarded as relatively uniform in space. In the case of catchment 24 (second column in Figure 3) and especially in the case of catchment 27 (third column in Figure 3), major differences arise from the two methods. Both catchments exhibit very variable patterns in the hillslope distance to the nearest channel. Remarkably, however, it appears that a scaling relation between A_N and A_T can still be found and that allows a fair determination of the scaling exponent b_A. In the case of catchment 27, the exponents b_G obtained with the two DEM of different resolution were very similar but relatively different for the exponent b_A, see Table 2. The values computed with the 5 m resolution DEM have been used in the following for the catchment 27.

[15] The geomorphological exponents of the two conceptual models, b_G and b_A, have been compared to the recession exponents β of all the basins in Figures 4a and 4b, respectively. The horizontal uncertainty bars represent the standard deviation of the recession exponents β computed on a single event basis and the solid black line represents the one-to-one relation. The upper plot is visibly more scattered than the lower plot where the points are more aligned along the one to one line. More formally, a simple frequency distribution of the difference between the geomorphological exponents b_G and b_A and the median recession exponents β is presented in the insets of Figures 4a and 4b, respectively. With a mean residual of 0.20, it appears clearly that, on average, the exponent b_A obtained with the new method matches better the exponent β of the recession analysis than the exponent b_G obtained with the first method (mean residual of 0.67). The improvement of the new method is even more remarkable when the residuals are classified along mean basin altitudes, see color coding in Figure 5. For low-altitude basins (mean altitude below 1000 m, first line in green in Figure 5), the mean residuals decrease between the first and the second method. For the watersheds at medium mean altitudes (mean altitude between 1000 and 2000 m in red in Figure 5) and especially for watersheds at high mean altitudes (mean altitude above 2000 m in blue in Figure 5), the new method improves the results with a larger decrease in the mean residual. Assuming increasing spatial complexity of the channel network with mean basin altitude, our results suggest that the proposed revised method provides better results in catchments where local drainage density is naturally heterogeneous reflecting the variety of channel initiation processes (i.e., proglacial, high-altitude catchments). In the case of low-

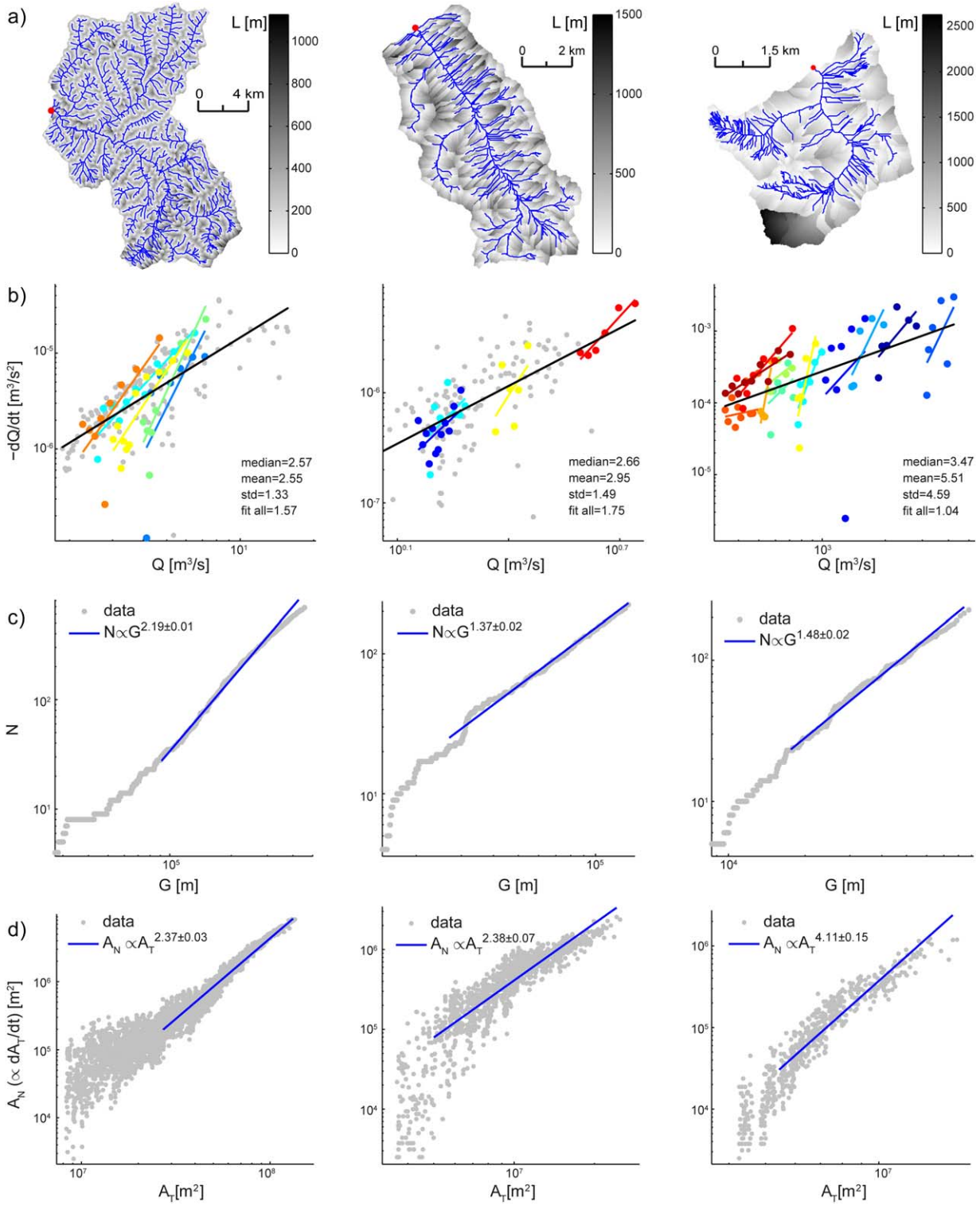

Figure 3. Example of the results obtained for watershed 15 (column 1), watershed 24 (column 2), and watershed 27 (column 3), see basins characteristics in Table 1. The different lines correspond to (a) the channel network obtained with the area threshold method in blue and in black and white the distance L to the nearest channel following the steepest path (except for watershed 27, column 3 where the real, monitored network has been used), (b) the cloud of points in gray obtained from the recession analysis with some events and their fit represented in different colors. Note that only few events are presented in colors for better visibility, (c) number of sources $N(l)$ versus ADN length $G(l)$ from which we obtain the geomorphologic exponent b_G, and (d) total area draining directly in all sources of the ADN A_N versus total area draining directly in the ADN A_T from which we obtain the geomorphologic exponent b_A.

Table 2. Summary of the Results Obtained From the Recession Analysis (Exponent β), From the Model Comparing N Versus G (Geomorphological Exponent b_G) and From the Model Comparing A_N Versus A_T (Geomorphological Exponent b_A) and Their Respective Residuals Compared to β

	Number of Events	Coefficient β for All Events Together	Median Coefficient β for Separated Events	Mean Coefficient β for Separated Events	Standard Deviation of β	b_G (N Versus G)	Residuals Median β-b_G	b_A (A_N versus A_T)	Residuals Median β-b_A
1	30	1.75	2.58	2.70	0.98	1.70 ± 0.01	0.87	1.56 ± 0.03	1.02
2	36	2.21	3.28	3.27	0.80	1.69 ± 0.01	1.59	1.99 ± 0.03	1.29
3	30	1.66	2.16	2.12	0.65	1.75 ± 0.01	0.41	1.83 ± 0.07	0.34
4	23	1.24	1.96	1.83	0.51	2.21 ± 0.01	−0.25	2.82 ± 0.06	−0.86
5	59	1.73	2.54	2.80	1.06	1.89 ± 0.01	0.64	1.95 ± 0.03	0.59
6	25	2.55	6.24	6.96	4.52	2.45 ± 0.02	3.78	2.52 ± 0.09	3.71
7	19	1.03	2.54	3.26	2.28	1.80 ± 0.02	0.74	1.76 ± 0.11	0.78
8	19	1.73	2.35	2.26	0.87	2.21 ± 0.02	0.13	2.83 ± 0.07	−0.49
9	14	1.88	2.89	2.61	0.87	2.32 ± 0.02	0.56	2.49 ± 0.06	0.40
10	25	1.81	2.91	2.86	1.29	1.99 ± 0.01	0.91	2.64 ± 0.02	0.27
11	56	1.82	3.34	3.91	2.01	0.79 ± 0.09	2.56	1.12 ± 0.15	2.22
12	13	1.48	1.20	1.77	1.03	1.10 ± 0.06	0.11	1.55 ± 0.16	−0.35
13	36	1.15	2.20	2.17	0.86	1.42 ± 0.01	0.79	1.44 ± 0.08	0.76
14	44	1.80	2.28	2.55	1.23	2.03 ± 0.01	0.25	2.18 ± 0.02	0.11
15	20	1.57	2.57	2.55	1.33	2.19 ± 0.01	0.38	2.37 ± 0.03	0.20
16	23	1.87	2.39	2.70	1.05	1.60 ± 0.01	0.79	2.96 ± 0.04	−0.57
17	10	1.51	1.29	1.70	0.78	1.59 ± 0.01	−0.30	2.04 ± 0.05	−0.75
18	17	0.74	2.04	2.49	2.07	1.98 ± 0.01	0.06	2.87 ± 0.03	−0.83
19	12	1.42	2.86	3.01	1.23	1.36 ± 0.02	1.50	1.14 ± 0.08	−0.34
20	13	0.89	1.06	2.65	2.94	1.88 ± 0.01	−0.81	2.99 ± 0.12	0.29
21	25	1.73	2.73	3.63	3.16	1.94 ± 0.02	0.78	2.03 ± 0.06	0.70
22	14	0.59	1.31	1.32	0.59	1.02 ± 0.01	0.29	2.15 ± 0.13	−0.84
23	14	1.53	3.20	3.48	1.61	2.12 ± 0.08	1.07	3.53 ± 0.25	−0.34
24	18	1.75	2.66	2.95	1.49	1.37 ± 0.02	1.29	2.38 ± 0.07	0.29
25	40	1.79	3.90	4.29	3.18	1.37 ± 0.02	2.53	1.29 ± 0.09	2.62
26	11	1.72	2.82	2.81	1.79	1.62 ± 0.01	1.20	1.51 ± 0.09	1.31
27	12	1.05	3.47	5.51	4.59	1.48 ± 0.02[a]	1.99[a]	4.11 ± 0.15[a]	−0.64[a]
						1.53 ± 0.01[b]	1.94[b]	3.40 ± 0.04[b]	0.07[b]

[a]Results obtained with the 25 m resolution DEM.
[b]Results obtained with the 5 m resolution DEM.

altitude catchments, where local drainage density tends to be uniform in space, the two methods provide similar results.

5. Discussion

[16] We find that the discrepancies arising between the exponent β obtained from the analysis of the recession curves and the geomorphological parameter b_G obtained from the original method proposed in *Biswal and Marani* [2010] are relatively small for low-altitude basins but larger for higher altitude basins. Compared to the watersheds studied in *Biswal and Marani* [2010], the watersheds chosen in this study are probably less suited to the original conditions envisioned by *Brutsaert and Nieber* [1977]: they are relatively smaller, structurally inconsistent with the conceptual model of simple drainage of an unconfined aquifer and generally exhibiting faster responses to rainfall impulses especially due to steep hillslopes. Often, as highlighted in the physical features of Table 1, the catchment response shows signatures of snow or ice melt, both leading to larger uncertainties in the evaluation of the recession exponent β. Moreover, such discrepancy is very large in the case of an urbanized watershed (basin 6 in Tables 1 and 2), confirming that the method is mostly suited to watersheds with little anthropogenic influence. However, the discrepancies between b_G and β cannot be explained only by the uncertainty in the exponent β, and some assumptions made by the method must be relaxed when hydrologic and geomorphic conditions required are not met.

[17] Our proposed correction of the method indeed accounts for uneven local drainage density, because it assumes that the local contributing discharge per unit length of receding ADN is limited by the local hillslope to channel distance and its directly contributing area. This is typically occurring in high altitude, proglacial dominated catchments where channel initiation processes are most diverse and unchanneled distances may vary from tens to thousands of meters. The inclusion aims at improving our understanding of the geomorphological origin of the recession curves, as noted in section 3. The system is described by the evolution in time of A_T, the area draining directly into the ADN relative to the area A_N draining into the sources of the ADN, leading to an empirical relation $A_N \propto {A_T}^{b_A}$. Our results suggest that the new geomorphological parameter b_A is closer to the exponent β, resulting in a decrease of the residuals between the two exponents (Figure 4). In particular, the correction is substantial in the Val Ferret catchment (number 27) where the real, monitored network has been used for the calculations. For this high-altitude catchment, endowed with highly uneven local drainage density, the residuals between the exponents $\beta - b_G$ and $\beta - b_A$ decrease from 1.99 to −0.64 and from 1.94 to 0.07 between the two methods for the 25 m resolution and the 5 m resolution DEM, respectively. In other particular cases where the local drainage density is more

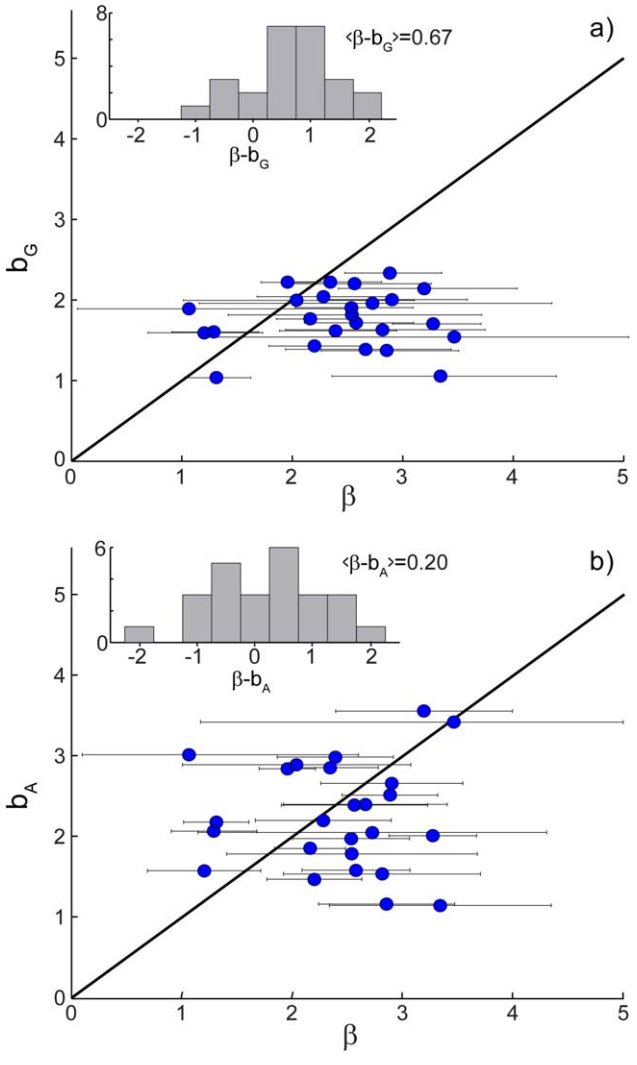

Figure 4. Recession exponent β versus geomorphological exponent for (a) b_G with the N versus G method and (b) b_A with the A_N versus A_T method. The insets in Figures 4a and 4b correspond to a simple frequency distribution of the residuals $\beta - b_G$ and $\beta - b_A$, respectively.

even, the two methods produce very similar results (see catchments 3, 5, or 7) and the two methods give comparable results as expected from the fact that the approaches tend to collapse into the same formulation.

[18] We acknowledge several sources of uncertainty introduced in the model, chiefly through the resolution of the DEM and through the area threshold method adopted for the channel network extraction (which is known to fail in complex terrain where heterogeneities of channel initiation processes are major). In the Val Ferret catchment, the uncertainty in the channel network extraction is dramatically decreased by an accurate field channel network monitoring resulting in improved results for the method proposed here. However, the time series available for measured streamflows for this watershed is less compared to the 26 others leading to a greater uncertainty in the exponent β. Field campaigns in other small watersheds aimed at monitoring channel initiations would probably improve the performance and the reliability of this conceptual model. In the Val Ferret catchment, our results were not affected by the DEM resolution since the geomorphological parameter b_A was closer to β than b_G to β in both DEM resolution cases. Therefore, the uncertainty introduced by the DEM resolution might only alter the accuracy of the predicted exponent but not the essence of our method. We also acknowledge larger uncertainties in the estimation of the parameter b_A due to the larger scatter in the A_N versus A_T plots which is the mark of uneven local drainage densities. We note, however, that the error in the estimate of the parameter b_A is still small compared to the error in the exponent β. Finally, we note that our study pinpoints that the most critical assumption of the conceptual model lies in neglecting the term dq/dt in equation (3) with respect to the change in the ADN geometry. Further studies are thus needed in order to combine the results of the method here formulated with a possibly geomorphically controlled integration, modeling the speed of the negative traveling wave of active stream switch offs.

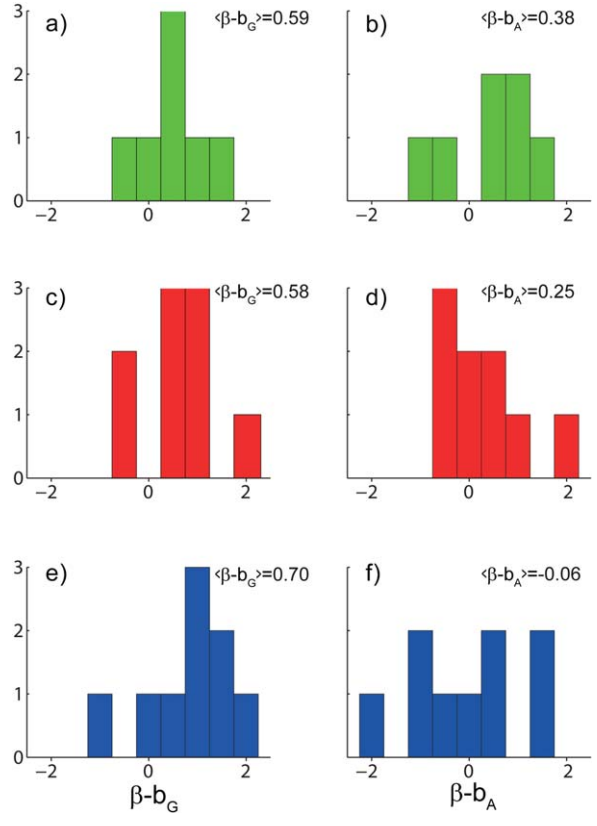

Figure 5. Histogram of the residuals between the recession exponent β and the geomorphological exponents (a, c, and e) b_G (left histograms) and (b, d, and f) b_A (right histograms) classified along mean basin altitude, from top to bottom in green (first row, Figures 5a and 5b) for basins at mean altitude below 1000 m, in red (Figures 5c and 5d) for basins at mean altitude between 1000 and 2000 m and in blue (Figures 5e and 5f) for basins at mean altitude above 2000 m.

6. Concluding Remarks

[19] Catchment recession curves bear the signatures of geomorphology. Two conceptual models based on empirical relations obtained solely from the analysis of DEMs have been compared. Both models describe the impact of geomorphology on the recession curves of the stream network, described in the first model by the evolution of the number of sources in the active channel network versus the total active channel network length, and in the latter by the area draining in the sources of the receding network versus the total area draining directly in the network. From the analysis of 27 catchments relatively unaffected by anthropogenic influence, our results suggest that the two models give similar results in the cases where local drainage density is approximately constant. In the cases of spatially uneven local drainage density, the first model does not hold and the new model presented here improves the results for high-altitude basins. In general, we suggest that this conceptual model might be useful to estimate the low flow regime of natural ungauged basins by predicting its features solely from information remotely acquired and objectively manipulated through DEM data.

[20] **Acknowledgments.** The authors are grateful to the Swiss National Science Foundation for financial support (grant 200021_ 134982/1 and 200021-124930/1), to ERC Advanced Grant RINEC 226712 and to the NCCR-MICS and CCES fundings. The authors wish to thank the Commune d'Orsières for providing logistic support for the field campaigns in the Val Ferret catchment.

References

Bertuzzo, E., A. Maritan, M. Gatto, I. Rodriguez-Iturbe, and A. Rinaldo (2007), River networks and ecological corridors: Reactive transport on fractals, migration fronts, hydrochory, *Water Resour. Res.*, *43*, W04419, doi:10.1029/2006WR005533.

Biswal, B., and M. Marani (2010), Geomorphological origin of recession curves, *Geophys. Res. Lett.*, *37*, L24403, doi:10.1029/2010GL045415.

Biswal, B., and D. Nagesh Kumar (2012), Study of dynamic behaviour of recession curves, *Hydrol. Processes*, doi:10.1002/hyp.9604, in press.

Botter, G., F. Peratoner, A. Porporato, I. Rodriguez-Iturbe, and A. Rinaldo (2007a), Signatures of large-scale soil moisture dynamics on streamflow statistics across U.S. climate regimes, *Water Resour. Res.*, *43*, W11413, doi:10.1029/2007WR006162.

Botter, G., A. Porporato, E. Daly, I. Rodriguez-Iturbe, and A. Rinaldo (2007b), Probabilistic characterization of base flows in river basins: Roles of soil, vegetation, and geomorphology, *Water Resour. Res.*, *43*, W06404, doi:10.1029/2006WR005397.

Botter, G., A. Porporato, I. Rodriguez-Iturbe, and A. Rinaldo (2009), Nonlinear storage-discharge relations and catchment streamflow regimes, *Water Resour. Res.*, *45*, W10427, doi:10.1029/2008WR007658.

Botter, G., E. Bertuzzo, and A. Rinaldo (2010), Transport in the hydrologic response: Travel time distributions, soil moisture dynamics, and the old water paradox, *Water Resour. Res.*, *46*, W03514, doi:10.1029/2009WR008371.

Boussinesq, J. (1903), Sur le débit, en temps de sécheresse, d'une source alimentée par une nappe d'eaux d'infiltration, *C. R. Hebd. Seances. Acad. Sci.*, *136*, 1511–1517.

Boussinesq, J. (1904), Recherches théoriques sur l'écoulement des nappes d'eau infiltrées dans le sol et sur débit de sources, *J. Math. Pure Appl.*, *10*, 5–78.

Brutsaert, W. (2008), Long-term groundwater storage trends estimated from streamflow records: Climatic perspective, *Water Resour. Res.*, *44*, W02409, doi:10.1029/2007WR006518.

Brutsaert, W., and T. Hiyama (2012), The determination of permafrost thawing trends from long-term streamflow measurements with an application in eastern Siberia, *J. Geophys. Res.*, *117*, D22110, doi:10.1029/2012JD018344.

Brutsaert, W., and J. P. Lopez (1998), Basin-scale geohydrologic drought flow features of riparian aquifers in the Southern Great Plains, *Water Resour. Res.*, *34*(2), 233–240, doi:10.1029/97WR03068.

Brutsaert, W., and J. L. Nieber (1977), Regionalized drought flow hydrographs from a mature glaciated plateau, *Water Resour. Res.*, *13*(3), 637–643, doi:10.1029/WR013i003p00637.

Brutsaert, W., and M. Sugita (2008), Is Mongolia's groundwater increasing or decreasing? The case of the Kherlen River basin/Les eaux souterraines de Mongolie s'accroissent ou décroissent-elles? Cas du bassin versant la Rivière Kherlen, *Hydrol. Sci. J.*, *53*(6), 1221–1229, doi:10.1623/hysj.53.6.1221.

Ceola, S., G. Botter, E. Bertuzzo, A. Porporato, I. Rodriguez-Iturbe, and A. Rinaldo (2010), Comparative study of ecohydrological streamflow probability distributions, *Water Resour. Res.*, *46*, W09502, doi:10.1029/2010WRr009102.

Eng, K., and W. Brutsaert (1999), Generality of drought flow characteristics within the Arkansas River basin, *J. Geophys. Res.*, *104*(D16), 19,435–19,441, doi:10.1029/1999JD900087.

Harman, C. J., M. Sivapalan, and P. Kumar (2009), Power law catchment-scale recessions arising from heterogeneous linear small-scale dynamics, *Water Resour. Res.*, *45*, W09404, doi:10.1029/2008WR007392.

Horton, R. E. (1932), Drainage basin characteristics, *Trans. AGU*, *13*, 350–361, doi:10.1029/TR013i001p00350.

Horton, R. E. (1945), Erosional development of streams and their drainage basins; hydrophysical approach to quantitative morphology, *Geol. Soc. Am. Bull.*, *56*(3), 275–370, doi:10.1130/0016–7606(1945)56[275:edosat]2.0.co;2.

Kirchner, J. W. (2009), Catchments as simple dynamical systems: Catchment characterization, rainfall-runoff modeling, and doing hydrology backward, *Water Resour. Res.*, *45*, W02429, doi:10.1029/2008WR006912.

Kondolf, G. M., L. M. Maloney, and J. G. Williams (1987), Effects of bank storage and well pumping on base flow, Carmel River, Monterey County, California, *J. Hydrol.*, *91*(3–4), 351–369, doi:10.1016/0022–1694(87)90211-3.

Malvicini, C. F., T. S. Steenhuis, M. T. Walter, J. Y. Parlange, and M. F. Walter (2005), Evaluation of spring flow in the uplands of Matalom, Leyte, Philippines, *Adv. Water Resour.*, *28*(10), 1083–1090, doi:10.1016/j.advwatres.2004.12.006.

Marani, M., E. Belluco, A. D'Alpaos, A. Defina, S. Lanzoni, and A. Rinaldo (2003), On the drainage density of tidal networks, *Water Resour. Res.*, *39*(2), 1040, doi:10.1029/2001WR001051.

McMillan, H. K., M. P. Clark, W. B. Bowden, M. Duncan, and R. A. Woods (2011), Hydrological field data from a modeller's perspective: Part 1. Diagnostic tests for model structure, *Hydrol. Processes*, *25*(4), 511–522, doi:10.1002/hyp.7841.

Mendoza, G. F., T. S. Steenhuis, M. T. Walter, and J. Y. Parlange (2003), Estimating basin-wide hydraulic parameters of a semi-arid mountainous watershed by recession-flow analysis, *J. Hydrol.*, *279*(1–4), 57–69, doi:10.1016/s0022–1694(03)00174-4.

Montgomery, D. R., and W. E. Dietrich (1988), Where do channels begin?, *Nature*, *336*(6196), 232–234, doi:10.1038/336232a0.

Montgomery, D. R., and W. E. Dietrich (1992), Channel initiation and the problem of landscape scale, *Science*, *255*(5046), 826–830, doi:10.1126/science.255.5046.826.

Montgomery, D. R., and E. Foufoula-Georgiou (1993), Channel network source representation using digital elevation models, *Water Resour. Res.*, *29*(12), 3925–3934, doi:10.1029/93WR02463.

O'Callaghan, J. F., and D. M. Mark (1984), The extraction of drainage networks from digital elevation data, *Comput. Vision Graphics Image Process.*, *28*(3), 323–344, doi:10.1016/s0734-189x(84)80011-0.

Palmroth, S., G. G. Katul, D. Hui, H. R. McCarthy, R. B. Jackson, and R. Oren (2010), Estimation of long-term basin scale evapotranspiration from streamflow time series, *Water Resour. Res.*, *46*, W10512, doi:10.1029/2009WR008838.

Parlange, J. Y., F. Stagnitti, A. Heilig, J. Szilagyi, M. B. Parlange, T. S. Steenhuis, W. L. Hogarth, D. A. Barry, and L. Li (2001), Sudden drawdown and drainage of a horizontal aquifer, *Water Resour. Res.*, *37*(8), 2097–2101, doi:10.1029/2000WR000189.

Polubarinova-Kochina, P. Y. (1962), *Theory of Ground Water Movement*, 613 pp., Princeton Univ. Press, Princeton, N. J.

Rinaldo, A., W. E. Dietrich, R. Rigon, G. K. Vogel, and I. Rodriguez-lturbe (1995a), Geomorphological signatures of varying climate, *Nature*, *374*(6523), 632–635, doi:10.1038/374632a0.

Rinaldo, A., G. K. Vogel, R. Rigon, and I. Rodriguez-Iturbe (1995b), Can one gauge the shape of a basin?, *Water Resour. Res.*, *31*(4), 1119–1127, doi:10.1029/94WR03290.

Rinaldo, A., G. Botter, E. Bertuzzo, A. Uccelli, T. Settin, and M. Marani (2006), Transport at basin scales: 1. Theoretical framework, *Hydrol. Earth Syst. Sci.*, *10*(1), 19–29, doi:10.5194/hess-10–19-2006.

Rinaldo, A., K. Beven, E. Bertuzzo, L. Nicotina, J. Davies, A. Fiori, D. Russo, and G. Botter (2011), Catchment travel time distributions and water flow in soils, *Water Resour. Res.*, *47*, W07537, doi:10.1029/2011WR010478.

Rodriguez-Iturbe, I., and A. Rinaldo (2001), *Fractal River Basins: Chance and Self-Organization*, 547 pp., Cambridge Univ. Press, Cambridge, U. K.

Rodriguez-Iturbe, I., R. Muneepeerakul, E. Bertuzzo, S. A. Levin, and A. Rinaldo (2009), River networks as ecological corridors: A complex systems perspective for integrating hydrologic, geomorphologic, and ecologic dynamics, *Water Resour. Res.*, *45*, W01413, doi:10.1029/2008WR007124.

Rupp, D. E., and J. S. Selker (2006a), On the use of the Boussinesq equation for interpreting recession hydrographs from sloping aquifers, *Water Resour. Res.*, *42*, W12421, doi:10.1029/2006WR005080.

Rupp, D. E., and J. S. Selker (2006b), Information, artifacts, and noise in dQ/dt – Q recession analysis, *Adv. Water Resour.*, *29*(2), 154–160, doi:10.1016/j.advwatres.2005.03.019.

Rupp, D. E., J. M. Owens, K. L. Warren, and J. S. Selker (2004), Analytical methods for estimating saturated hydraulic conductivity in a tile-drained field, *J. Hydrol.*, *289*(1–4), 111–127, doi:10.1016/j.jhydrol.2003.11.004.

Rupp, D. E., J. Schmidt, R. A. Woods, and V. J. Bidwell (2009), Analytical assessment and parameter estimation of a low-dimensional groundwater model, *J. Hydrol.*, *377*(1–2), 143–154, doi:10.1016/j.jhydrol.2009.08.018.

Shaw, S. B., and S. J. Riha (2012), Examining individual recession events instead of a data cloud: Using a modified interpretation of dQ/dt–Q streamflow recession in glaciated watersheds to better inform models of low flow, *J. Hydrol.*, *434–435*, 46–54, doi:10.1016/j.jhydrol.2012.02.034.

Simoni, S., S. Padoan, D. F. Nadeau, M. Diebold, A. Porporato, G. Barrenetxea, F. Ingelrest, M. Vetterli, and M. B. Parlange (2011), Hydrologic response of an alpine watershed: Application of a meteorological wireless sensor network to understand streamflow generation, *Water Resour. Res.*, *47*, W10524, doi:10.1029/2011WR010730.

Sofia, G., P. Tarolli, F. Cazorzi, and G. Dalla Fontana (2011), An objective approach for feature extraction: Distribution analysis and statistical descriptors for scale choice and channel network identification, *Hydrol. Earth Syst. Sci.*, *15*(5), 1387–1402, doi:10.5194/hess-15–1387-2011.

Szilagyi, J., and M. B. Parlange (1998), Baseflow separation based on analytical solutions of the Boussinesq equation, *J. Hydrol.*, *204*(1–4), 251–260, doi:10.1016/S0022–1694(97)00132-7.

Szilagyi, J., and M. B. Parlange (1999), A geomorphology-based semi-distributed watershed model, *Adv. Water Resour.*, *23*(2), 177–187, doi:10.1016/S0309–1708(99)00021-4.

Szilagyi, J., M. B. Parlange, and J. D. Albertson (1998), Recession flow analysis for aquifer parameter determination, *Water Resour. Res.*, *34*(7), 1851–1857, doi:10.1029/98WR01009.

Tague, C., and G. E. Grant (2004), A geological framework for interpreting the low-flow regimes of Cascade streams, Willamette River Basin, Oregon, *Water Resour. Res.*, *40*, W04303, doi:10.1029/2003WR002629.

Tallaksen, L. M. (1995), A review of baseflow recession analysis, *J. Hydrol.*, *165*(1–4), 349–370, doi:10.1016/0022–1694(94)02540-r.

Tarboton, D. G., R. L. Bras, and I. Rodriguez-Iturbe (1991), On the extraction of channel networks from digital elevation data, *Hydrol. Processes*, *5*(1), 81–100, doi:10.1002/hyp.3360050107.

Tarolli, P., and G. Dalla Fontana (2009), Hillslope-to-valley transition morphology: New opportunities from high resolution DTMs, *Geomorphology*, *113*(1–2), 47–56, doi:10.1016/j.geomorph.2009.02.006.

Thompson, S. E., and G. G. Katul (2012), Multiple mechanisms generate Lorentzian and $1/f\alpha$ power spectra in daily stream-flow time series, *Adv. Water Resour.*, *37*, 94–103, doi:10.1016/j.advwatres.2011.10.010.

Tobin, C., B. Schaefli, L. Nicotina, S. Simoni, G. Barrenetxea, R. Smith, M. B. Parlange, and A. Rinaldo (2013), Improving the degree-day method for sub-daily melt simulations with physically-based diurnal variations, *Adv. Water Resour.*, *55*, 149–164, doi:10.1016/j.advwatres.2012.08.008.

Troch, P. A., F. P. De Troch, and W. Brutsaert (1993), Effective water table depth to describe initial conditions prior to storm rainfall in humid regions, *Water Resour. Res.*, *29*(2), 427–434, doi:10.1029/92WR02087.

Tucker, G. E., F. Catani, A. Rinaldo, and R. L. Bras (2001), Statistical analysis of drainage density from digital terrain data, *Geomorphology*, *36*(3–4), 187–202, doi:10.1016/S0169–555X(00)00056-8.

Vogel, R. M., and C. N. Kroll (1992), Regional geohydrologic-geomorphic relationships for the estimation of low-flow statistics, *Water Resour. Res.*, *28*(9), 2451–2458, doi:10.1029/92WR01007.

Wang, D., and X. Cai (2010), Recession slope curve analysis under human interferences, *Adv. Water Resour.*, *33*(9), 1053–1061, doi:10.1016/j.advwatres.2010.06.010.

Weijs, S. V., R. Mutzner, and M. B. Parlange (2013), Could electrical conductivity replace water level in rating curves for alpine streams?, *Water Resour. Res.*, *49*(1), 343–351, doi:10.1029/2012WR012181.

Wittenberg, H. (1999), Baseflow recession and recharge as nonlinear storage processes, *Hydrol. Processes*, *13*(5), 715–726, doi:10.1002/(sici)1099-1085(19990415)13:5<715::aid-hyp775>3.0.co;2-n.

Zaliapin, I., E. Foufoula-Georgiou, and M. Ghil (2010), Transport on river networks: A dynamic tree approach, *J. Geophys. Res.*, *115*, F00A15, doi:10.1029/2009JF001281.

Zecharias, Y. B., and W. Brutsaert (1988), Recession characteristics of groundwater outflow and base flow from mountainous watersheds, *Water Resour. Res.*, *24*(10), 1651–1658, doi:10.1029/WR024i010p01651.